

NASA TP-2012-XX



Probability of Causation for Space Radiation Carcinogenesis following ISS, NEA and Mars Missions

Francis A. Cucinotta

*NASA Lyndon B. Johnson Space Center
Houston, Texas*

*Myung-Hee Y. Kim and Lori J. Chappell
U.S.R.A., Division of Space Life Sciences
Houston, Texas*

THE NASA STI PROGRAM OFFICE . . . IN PROFILE

Since its founding, NASA has been dedicated to the advancement of aeronautics and space science. The NASA Scientific and Technical Information (STI) Program Office plays a key part in helping NASA maintain this important role.

The NASA STI Program Office is operated by Langley Research Center, the lead center for NASA's scientific and technical information. The NASA STI Program Office provides access to the NASA STI Database, the largest collection of aeronautical and space science STI in the world. The Program Office is also NASA's institutional mechanism for disseminating the results of its research and development activities. These results are published by NASA in the NASA STI Report Series, which includes the following report types:

- **TECHNICAL PUBLICATION.** Reports of completed research or a major significant phase of research that present the results of NASA programs and include extensive data or theoretical analysis. Includes compilations of significant scientific and technical data and information deemed to be of continuing reference value. NASA's counterpart of peer-reviewed formal professional papers but has less stringent limitations on manuscript length and extent of graphic presentations.
- **TECHNICAL MEMORANDUM.** Scientific and technical findings that are preliminary or of specialized interest, e.g., quick release reports, working papers, and bibliographies that contain minimal annotation. Does not contain extensive analysis.
- **CONTRACTOR REPORT.** Scientific and technical findings by NASA-sponsored contractors and grantees.

- **CONFERENCE PUBLICATION.** Collected papers from scientific and technical conferences, symposia, seminars, or other meetings sponsored or cosponsored by NASA.
- **SPECIAL PUBLICATION.** Scientific, technical, or historical information from NASA programs, projects, and mission, often concerned with subjects having substantial public interest.
- **TECHNICAL TRANSLATION.** English-language translations of foreign scientific and technical material pertinent to NASA's mission.

Specialized services that complement the STI Program Office's diverse offerings include creating custom thesauri, building customized databases, organizing and publishing research results . . . even providing videos.

For more information about the NASA STI Program Office, see the following:

- Access the NASA STI Program Home Page at <http://www.sti.nasa.gov>
- E-mail your question via the Internet to help@sti.nasa.gov
- Fax your question to the NASA Access Help Desk at (301) 621-0134
- Telephone the NASA Access Help Desk at (301) 621-0390
- Write to:
NASA Access Help Desk
NASA Center for AeroSpace Information
7121 Standard
Hanover, MD 21076-1320

NASA/TP-2012-XX



Probability of Causation of Space Radiation Carcinogenesis following ISS, NEA and Mars Missions

Francis A. Cucinotta

NASA Lyndon B. Johnson Space Center

Houston, Texas

Myung-Hee Y. Kim and Lori J. Chappell

U.S.R.A., Division of Space Life Sciences

Houston, Texas

Pre-Print

Available from:

NASA Center for AeroSpace Information
7121 Standard Drive
Hanover, MD 21076-1320

National Technical Information Service
5285 Port Royal Road
Springfield, VA 22161

This report is also available in electronic form at <http://ston.jsc.nasa.gov/collections/TRS>

Table of Contents

Glossary	v
Abstract.....	vii
1. Introduction.....	1
2. Cancer Risk Projection Model	3
3. Space Radiation and Organ Exposures	6
4. Uncertainty Analysis.....	12
5. Results.....	15
6. Discussion and Conclusions	20
7. References.....	22

Glossary

ALARA	as low as reasonably achievable
AR	Attributable Risk
BEIR	(NAS) Committee on the Biological Effects of Ionizing Radiation
BRYNTRN	baryon transport computer code
CDC	Center for Disease Control
CI	confidence intervals
CL	confidence level
CNS	central nervous system
DDREF	dose and dose-rate reduction effectiveness factor
D_r	dose-rate (Gy/hr)
EAR	excess additive risk, Sv^{-1}
ERR	excess relative risk, $Sv^{-1} yr^{-1}$
EVA	extra-vehicular activity
F	fluence (number of ions per unit area) no. ions/cm ²
GCR	galactic cosmic rays
GM	geometric mean
GSD	geometric standard deviation
HZE	high-energy and charge
HZETRN	high charge and energy transport computer code
ICRP	International Commission on Radiological Protection
ISS	International Space Station
LEO	low Earth orbit
LET	linear energy transfer, keV/ μm
LSS	Life-Span Study of the Japanese atomic-bomb survivors
NEA	Near Earth Asteroid
NRC	National Research Council
NS	Never-smoker (lifetime use less than 100 cigarettes)
NSRL	NASA Space Radiation Laboratory
NTE	Non-Targeted Effect
PC	Probability of Causation
PDF	probability distribution function
Q	quality factor
$Q(L)$	quality factor as a function of linear energy transfer
$Q_{leukemia}$	quality factor for estimating leukemia risks
Q_{solid}	quality factor for estimating solid cancer risks
QMSFRG	quantum multiple scattering fragmentation model
RBE	relative biological effectiveness
RBE_{max}	maximum relative biological effectiveness that assumes linear responses at low doses or dose-rates
REIC	risk of exposure-induced cancer incidence

REID	risk of exposure-induced death
RERF	Radiation Effects Research Foundation
SD	standard deviation
SEER	surveillance, epidemiology, and end results
SPE	solar particle event
w_T	Tissue weighting factor
x_{Tr}	track structure scaling parameter equivalent to Z^*/β^2
x_α	quantiles (random variables) associated with factor α
UNSCEAR	United Nations Special Committee on the Effects of Atomic Radiation
Z	Charge number
Z^*	Effective charge number
α	Coefficient of linear dose response term, Gy^{-1}
$\phi_j(x, E)$	number of particles of type j with energy, E at depth, x in shielding, $1/(MeV/u\ cm^2)$
λ_j	gender and age-specific cancer incidence rate, cancers/yr
κ	Parameter in action cross section to determine most biologically effects Z^{*2}/β^2
Σ	Track structure derived risk cross section, μm^2

Abstract:

Cancer risk is an important concern for International Space Station (ISS) missions and future exploration missions to Mars and other destinations. As space programs mature an important question arises as to the likelihood of a causal association between a crew-members' radiation exposure and the occurrence of cancer. The probability of causation (PC), also denoted as attributable risk (AR), is used to make such an estimate. PC estimates above 50% suggests an observed cancer was more likely to be attributed to radiation exposure than not. Because of the uncertainties in estimating radiation cancer risks, analysis of terrestrial occupational exposure risk has estimated PC at the 95th or 99th percentile confidence levels (CL) in assessing the possible relationship between prior radiation exposures and cancer. In this report, we first summarize the NASA model of space radiation cancer risks and uncertainties, including improvements to represent uncertainties in tissue specific cancer incidence models for never-smokers (NS) and the U.S. average population. We then report on tissue specific cancer incidence estimates and PC for different post-mission times for ISS and exploration missions. Results show that leukemia and stomach cancer are most likely related to space radiation exposures followed by lung, colon, bladder, and liver cancers. PC estimates for a single ISS mission are not found to exceed 50% even at the 95% CL. However, median PC and 95%-CL are found to exceed 50% for many cancer types for deep space missions. PC estimates for NS are estimated to be increased compared to an U.S. average population for lung and several other tissues, although absolute risks are reduced for NS compared to the U.S. average population. An important conclusion from our analysis is that the NASA policy to limit the risk of exposure induced death (REID) to 3% at the 95% CL largely ensures that estimates of the PC for most cancer types would not reach a level of significance. Reducing uncertainties through radiobiological research remains the most efficient method to extend mission length and establish effective mitigator's for cancer risks. Efforts to establish biomarkers of space radiation induced tumors and to estimate PC for rarer tumor types are briefly discussed.

1. Introduction

In this paper we discuss methods to estimate the probability of causation (PC) also known as Attributable Risk (AR) for space radiation exposures. Astronauts are exposed to galactic cosmic rays (GCR) — made up of high-energy protons and high-energy and charge (HZE) nuclei, and solar particle events (SPEs) — comprised largely of low- to medium-energy protons, which are a critical challenge for space exploration. Experimental studies have shown that HZE nuclei produce both qualitative and quantitative differences in biological effects compared to terrestrial radiation (reviewed in NAS, 1996; Cucinotta and Durante, 2006; Durante and Cucinotta, 2008; Schimmerling *et al.*, 1999; NCRP, 2006) leading to large uncertainties in predicting exposure health outcomes to humans. The uncertainties in estimating GCR health risks are a major limitation to the length of space missions and the evaluation of potential risk mitigator's. NASA limits astronaut exposures to a 3% risk of exposure induced death (REID), and protects against uncertainties in risks projections using an assessment of 95% confidence intervals of risk estimates (Cucinotta *et al.*, 2011). Beyond efforts related to risk limitation prior to a mission, there will also be a concern for cancers observed in crew members at post-mission and their possible association with prior space radiation exposures. The PC is a conditional probability of risk used as an indicator of a potential causal relationship between radiation exposure and occurrence of cancer in a population. The calculation of PC with concomitant uncertainty analysis will allow NASA to make estimates that an observed cancer was caused by occupational exposure, however should be augmented with considerations of an individual's family history of disease, possible exposure to other carcinogens, and of individual based biomarkers.

Astronauts and other healthy workers enjoy many lifestyle factors that lead to reduced lifetime cancer risks compared to the U.S. average population (Calle *et al.*, 1999). Healthy worker attributes found for astronauts include optimal ranges of body mass index (BMI), moderate alcohol use, excellent nutrition and exercise regimes, and health care (LSAH 2003). More importantly, more than 90% of astronauts are never-smokers (NS) and therefore are expected to have lower background cancer rates than the U.S. average rates, which include current and former smokers along with never-smokers. It is well known that NS have lower rates of cancer, circulatory and pulmonary diseases, and longer life-span than former or current smokers (Thun *et al.*, 1995; Doll *et al.*, 2004). Indeed, more than 20% of all deaths in the US are associated with tobacco exposure, including over 80% of all lung cancer deaths (CDC-MMWR 2010). In addition epidemiology studies suggest a harmful synergistic interaction between radiation and tobacco exposure occurs (Gilbert *et al.*, 2003; Furukawa *et al.*, 2010; Leuraud *et al.*, 2011; Cucinotta *et al.*, 2012). Not all lifestyle factors typical of astronauts are favorable for lowering cancer risks, where for example higher wages compared to U.S. median wages, are reported to be associated with increase cancer risk (CDC 2008) however a smaller effect than for example tobacco use. Exposure to second-hand smoke would be variable in the astronaut or other healthy populations, and can significantly increase lung cancer and circulatory disease risk (CDC-MMWR 2010). Radiation risk estimates have used models based on the U.S. average population (NCRP, 2000) until recently (Cucinotta and Chappell, 2011). Because cancer risk estimates are made using a mixture of multiplicative and additive risk transfer models, the lower background cancer rates of a healthy population reduce radiation risk estimates compared to estimates for the U.S. average population (Cucinotta *et al.* 2011, 2012). In this report, we show that the opposite effect will occur for the conditional probability represented by the PC; whereby the PC is increased for several radiogenic cancers for a NS population compared to the U.S. average population.

Figure 1. Kaplan-Meier survival versus age for Astronauts and payload specialists compared to U.S. males and our projections for NS males. The left panel includes occupational deaths related to flight accidents or training, and right panel censors occupational deaths. Data from the Astronaut Fact Book (NASA 2005) and <http://www.jsc.nasa.gov/Bios/>.

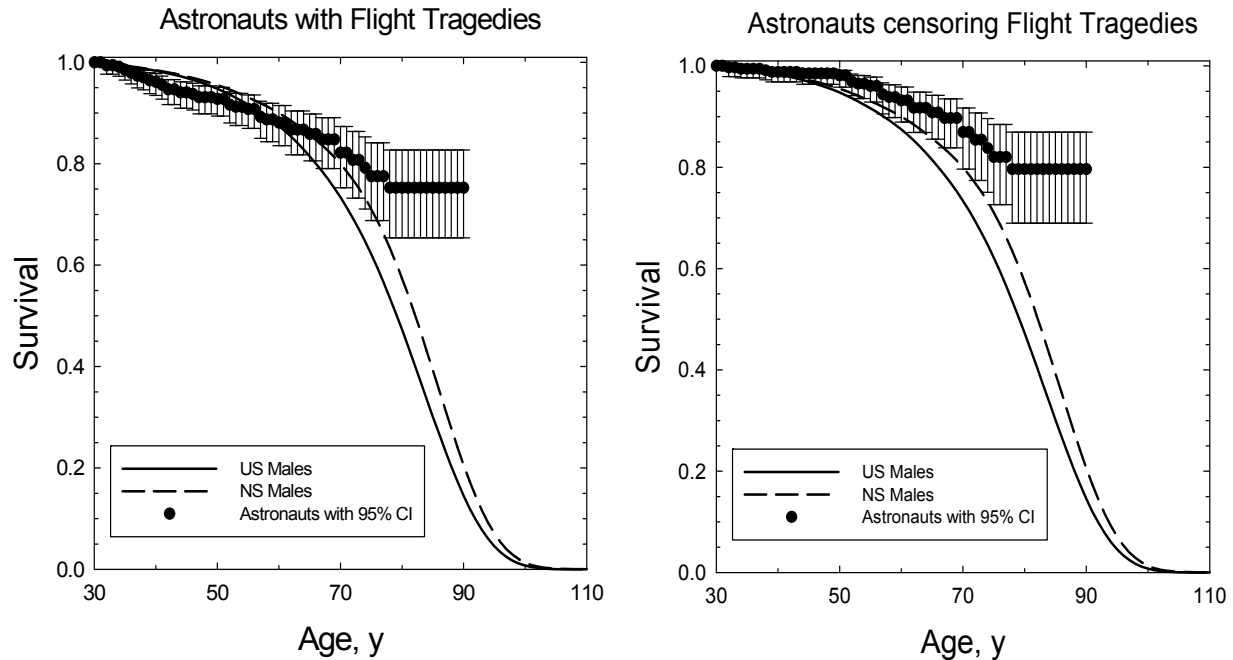


Table 1a. Statistics for fatalities amongst Astronauts and Payload specialists*.

<i>Category</i>	<i>Total Frequency</i>	<i>Death Frequency</i>
Male Astronauts	269	41
Female Astronauts	40	3
Total Astronaut	316	43
Payload Specialist	23	1
Total	339	44

*Causes of death were 10 cancers, 4 circulatory diseases, 1 CNS, 19 occupational accidental deaths, 4 non-occupational accidental deaths, and 5 other causes of death. Data from the Astronaut Fact Book (NASA 2005) and <http://www.jsc.nasa.gov/Bios/>.

Table 1b. Standard Mortality Ratio (SMR) for Astronauts and Payload Specialists relative to U.S. average or Never-smokers average (gender weighted to proportion of M and F astronauts) or female NS, suggests Astronauts have lifetime risks similar to female NS.

<i>Comparison</i>	<i>SMR</i>	<i>P-value</i>
Astronauts vs. U.S. avg.	0.67 [0.50, 0.90]	0.0006
Censoring tragedies vs. US avg.	0.40 [0.27, 0.58]	<10 ⁻⁶
Astronauts vs. NS avg.	0.88 [0.65, 1.18]	0.391
Censoring tragedies vs. NS avg.	0.52 [0.35, 0.76]	0.00067
Astronauts vs. Female NS	1.33 [0.99, 1.78]	0.0592
Censoring tragedies vs. Female NS	0.78 [0.53, 1.15]	0.215

Evidence that astronauts should be considered to be at lower risk for cancers and enjoy longer lifespan compared to the U.S. average population is borne out by analysis of Kaplan-Meier survival curves (**Figure 1**) and Standard Mortality Ratios (SMR) (**Table 1**), where the cohort of NASA astronauts and payload specialists is compared to the U.S. average population (CDC 2008) and the estimates for a NS population. These comparisons include results after censoring 18 of 19 occupationally related accidental deaths from space missions or training considered atypical of U.S. workers. The largely male cohort of astronauts and payload specialists show a longer longevity and reduced SMR in comparison to the U.S. average population, and are more similar to a population of female NS, which is a strong indication that a healthy worker effect occurs for astronauts. The population effective dose (over 90 Sv for the astronaut cohort (Cucinotta 2001; Cucinotta *et al.*, 2008)) is unlikely to have led to any increase in cancers at this time. We next discuss the NASA 2010 cancer risk assessment model (Cucinotta *et al.*, 2011) and its application to PC estimates for ISS and exploration missions. In the past, uncertainty analyses of PC estimates have been used to screen exposed persons for a potential causal relationship to an observed cancer, and in the determination of monetary compensation (NIH 2003; DHHS 2002). We describe point estimates and upper 95% confidence levels (CL) of the PC for 15 radiogenic tissue sites and a grouped “remainder” category representing other cancer sites. Predictions for missions to the ISS, near Earth asteroids (NEA) and Mars are described, including comparisons for different ages of exposure and disease diagnosis.

2. Cancer Risk Projection Model

The instantaneous cancer incidence or mortality rates, λ_I and λ_M , respectively are modeled as functions of dose D , or dose-rate D_r , gender, age at exposure a_E , and attained age a or latency L , which is the time after exposure $L=a-a_E$. The λ_I (or λ_M) is a sum over rates for each tissue that contributes to risk, λ_{IT} . These dependencies vary for each cancer type that could be increased by radiation exposure. The total risk of exposure induced cancer (REIC) is calculated by folding the instantaneous radiation cancer incidence-rate with the probability of surviving to time t , which is given by the survival function $S_0(t)$ for the background population times the probability for radiation cancer death at previous time, and then integrating over the remainder of a lifetime:

$$(1) \quad REIC(a_E, D) = \int_{a_E}^{\infty} dt \lambda_I(a, a_E, D) S_0(t) e^{-\int_{a_E}^t dz \lambda_M(z, a_E, D)}$$

where z is the dummy integration variable. After adjustment for low dose and dose-rates through the dose and dose-rate effectiveness factor (DDREF) and radiation quality, the tissue-specific, cancer incidence rate for an organ dose equivalent, H_T , can be written as a weighted average of the multiplicative and additive transfer models, often called a mixture model:

$$(2) \quad \lambda_{IT}(a_E, a, H_T) = [v_T ERR_T(a_E, a) \lambda_{0IT}(a) + (1 - v_T) EAR_T(a_E, a)] \frac{H_T}{DDREF}$$

where v_T is the tissue-specific transfer model weight, λ_{0IT} is the tissue-specific cancer incidence rate in the reference population, and where ERR_T and EAR_T are the tissue specific excess relative risk and excess additive risk per Sievert, respectively. The Hazard rates for cancer mortality λ_M are modeled with similar approaches following the BEIR VII report (2006). Tissue

Table 2. Tissue specific transfer weight v_T for multiplicative risk transfer. Additive risk transfer weight is then given by $1-v_T$. Values described on page 126 of NCRP Report No. 132 (2000), and from pages 275-276 of BEIR VII (2006).

<i>Tissue</i>	<i>NCRP No. 132</i>	<i>BEIR VII</i>	<i>NASA 2010</i>
Lung	0.5	0.3	0.5
Breast	0.5	0**	0**
Thyroid	0.5	1.0**	1.0**
stomach, colon, esophagus	0.5	0.7	0.7
liver,			
Leukemia	0.0	0.7	0.5
All Others	0.5	0.7	0.5

**Based on meta-analysis results described in BEIR VII.

weights assumed in the NASA 2010 model are shown in **Table 2** along with recommendations from other reports. In the NASA 2010 Model (Cucinotta and Chappell 2011; Cucinotta *et al.*, 2011), we used the UNSCEAR report fitted EAR and ERR models for most tissue sites with the results from Preston *et al.* (2007) for a few tissues not reported by UNSCEAR. UNSCEAR employed Poisson maximum-likelihood methods and Bayesian analysis to represent dosimetry errors to fit generalized ERR and EAR models to the LSS for cancer incidence for REIC. The ERR function fitted to the LSS data was:

$$(3) \quad ERR(a, a_E, L, D) = (\alpha D + \beta D^2) e^{\gamma D} \exp[\kappa_1 1_S + \kappa_2 \ln(a - a_E) + \kappa_3 \ln(a) + \kappa_4 \ln(a_E)]$$

with a similar form for the EAR function. A linear dose response model provided the best fits to the tissue specific cancer incidence data for solid cancers. For leukemia's the linear-quadratic model provided the best fit. The addition of the latency dependence, $L=a-a_E$, was significant for several tissues, including EAR models for colon, breast and non-melanoma skin cancer, and ERR and EAR functions for the category of all other solid cancer incidence. For breast and thyroid cancers the NASA 2010 models follows BEIR VII, which recommended the use of results from a meta-analysis of several exposed cohorts, replacing results from the LSS with additive transfer models used for breast cancer (Preston *et al.*, 2002) and multiplicative transfer models used for thyroid cancer (Ron *et al.*, 1995). For estimating cancer risks for low dose or dose-rate exposures, NCRP Report 132 (NCRP 2000) used a DDREF of 2. The BEIR VII Report, recommended a DDREF of 1.5 based on Bayesian analysis of the LSS data and a select group of mouse tumor studies. The NIH uses (NIH 2003) a values close to 1.75, which is the choice for the NASA 2010 model (Cucinotta and Chappell, 2011).

Adjusting U.S. Cancer Rates for Never-Smokers Cancer Estimates

We estimated gender-specific NS cancer rates to represent a reference population by using age specific rates for lung cancer and relative risk factors derived from literature searches for other cancers. Age and gender specific NS lung cancer rates were recently compiled by Thun *et al.* (2009) from an analysis of 13 cohorts and 22 cancer registries. These rates are used for our analysis of radiation lung cancer risks for NS. For other cancers, we use CDC estimates of proportions of cancer deaths for smokers (S) and former smokers (FS) in the U.S. population. CDC estimates (2010) of relative risks between these populations were used for cancers of the

esophagus, stomach, bladder, and oral cavity, and acute myeloid leukemia. We also considered other published sources for several tissue sites, which are liver, colorectal, and lymphomas (Liang *et al.*, 2009; Sandler *et al.*, 2003; IARC 1986). We estimated the fraction of cancers categorized in the “remainder” category based on the number of cases reported by Preston *et al.* (2007) for different cancer types related to smoking including pharynx, larynx, and pancreas. Cancer rates reported for the U.S. population are made-up of populations of smokers (S), former smokers (FS), and never-smokers (NS) with proportions f_S , f_{FS} , and f_{NS} , which leads to:

$$(4) \quad \lambda_{0T}(a) = f_S \lambda_{0T}^S(a) + f_{FS} \lambda_{0T}^{FS}(a) + f_{NS} \lambda_{0T}^{NS}(a)$$

The relative risks (RR) of S and FS compared to NS, RR_S and RR_{FS} , respectively are then used to compare rates for NS to the U.S. average rates,

$$(5) \quad \lambda_{0T}^{NS}(a) = \frac{\lambda_{0T}(a)}{(RR_S f_S + RR_{FS} f_{FS} + f_{NS})}$$

We used the 2005 U.S. population data from SEER (2006) and the CDC (2008) to represent the average U.S. population, and CDC estimates of fractions of populations for S, FS, and NS for males and females above age 40 y. The resulting estimates of RR for NS compared to the U.S. population are shown in **Table 3**. For never-smoker risk estimates, we considered their longer lifespan due to their reduced mortality for cancer, circulatory and pulmonary diseases. Age-specific rates for all causes of death for NS were not available and instead we considered the survival probability for the average U.S. population and made adjustments for the age and gender specific rates for these diseases (CDC 2008; Malarcher *et al.*, 2000). Here we modified the survival probability in Eq. (1) to adjust for lower rates for cancers, circulatory and pulmonary diseases that are also linked to tobacco use (CDC 2008).

Probability of Causation

The PC or attributable risk is the fraction of the incidence of a disease in a population (exposed and non-exposed) that is due to radiation exposure. Thus the PC represents the incidence of a disease in the population that would be eliminated if there were no radiation exposure. The PC is estimated from Eq. (1) by limiting the upper limit of integration to the date of disease diagnosis, a_{Diag} for both the exposed population and the reference population, with the PC defined in terms of the conditional tissue specific Excess Relative Risk (ERR) for each tissue:

$$(6) \quad PC = \frac{ERR(T, a_{Diag})}{1 + ERR(T, a_{Diag})}$$

where

$$(7) \quad ERR(T, a_{Diag}) = \frac{\int_{a_E}^{a_{Diag}} dt \lambda_{IT}(a, a_E, D) S_0(t) e^{-\int_{a_E}^t dz \lambda_M(z, a_E, D)}}{\int_{a_E}^{a_{Diag}} dt \lambda_{IT}(a, a_E, 0) S_0(t)} - 1$$

Table 3. Estimates of relative risks (RR) for Never-smokers (NS) compared to Average U.S. Population for several cancers related to both smoking and radiation exposure.

Males	<i>Relative Risk to Never-Smokers (NS)</i>			RR(NS/US)
	Current smokers	Former smokers	Never-smokers	
Esophagus	6.76	4.46	1	0.27
Stomach	1.96	1.47	1	0.71
Bladder	3.27	2.09	1	0.50
Oral Cavity	10.89	3.4	1	0.23
Liver	2.25	1.75	1	0.63
Colorectal	1.19	1.21	1	0.89
Leukemia	2	1.5	1	0.69
Remainder	4	2.5	1	0.43
Lung*	23.26	8.7	1	0.11
Females	Current smokers	Former smokers	Never-smokers	RR(NS/US)
Esophagus	7.75	2.79	1	0.35
Stomach	1.36	1.32	1	0.85
Bladder	2.22	1.89	1	0.65
Oral Cavity	5.08	2.29	1	0.46
Liver	2.25	1.75	1	0.67
Colorectal	1.28	1.23	1	0.88
Leukemia	2	1.5	1	0.74
Remainder	4	2.5	1	0.48
Lung*	12.69	4.53	1	0.23

*Lung data shown only for comparison, where risk calculations made using Age-specific rates described in the text. For males, current smokers, former smokers, and never-smokers are estimated at 24, 40, and 36% of the population above age 50 y. For females we use 18, 35, and 47% for these percentages (CDC-MMWR, 2010).

3. Space Radiation and Organ Exposures

For calculations of space radiation tissue specific cancer risks, Eq. (2) is used for the cancer incidence risk rate with the organ dose equivalent estimated using the HZETRN Code (Wilson *et al.*, 1994) with QMSFRG model cross sections and Badhwar-O'Neill GCR environment (Cucinotta, *et al.*, 2011). For GCR the use of risk assessment quantities based on absorbed dose is expected to have short-comings and instead the NASA 2010 derived radiation quality descriptors of biological effectiveness based on particle track structure and fluence that were then expressed as radiation quality factors (Cucinotta *et al.*, 2011). Here a cancer risk cross section representing the probability per particle is written as:

$$(8) \quad \Sigma(Z, E) = \Sigma_0 [P(Z, E) + \frac{\alpha_\gamma}{\Sigma_0} (1 - P(Z, E))L]$$

with

$$(9) \quad P(Z, E) = \left(1 - e^{-Z^{*2} / \kappa \beta^2}\right)^m$$

where the three parameters of the model (Σ_0 / α_γ , m , and κ) based on subjective estimates of results from radiobiology experiments. A radiation quality factor function is then found as:

$$(10) \quad Q_{NASA} = (1 - P(E, Z)) + \frac{6.24(\Sigma_0 / \alpha_\gamma)P(E, Z)}{LET}$$

The NASA quality factor depends on both particle charge number, Z and kinetic energy, E and not linear energy transfer, LET alone as assumed in the ICRP definition of quality factors (ICRP 1990; ICRP 2003; NCRP 2000). Distinct quality factors for estimating solid cancer and leukemia risk are used, Q_{solid} and $Q_{leukemia}$, respectively. The parameters that enter Eq.'s (8) to (10) have straight-forward biophysical interpretations: Σ_0 is the maximum value of the cross section, which is related to RBE_{max} for the most biologically effective particle types. m is the slope of the cross section for increasing ionization density. κ determines the saturation value of the cross section, where the RBE begins to decline due to "overkill" effects. α_γ is related to the initial slope of the gamma-ray dose response. Only the ratio Σ_0 / α_γ enters into model calculations, and not the individual values of these parameter. For solid cancer risks, radiobiology data is sparse. However, the largest RBE for HZE nuclei is in the range from 20 to 50 for solid tumors in rodents, and for chromosomal aberrations and mutations in human cells. A lower value is observed for leukemia (Weil *et al.*, 2009). This assumes a linear dose response at low particle dose, ignoring non-targeted effects (NTEs) or other possible mechanisms that would lead to deviation from linearity at low fluence. Calculations with the NASA 2010 model include uncertainty analysis through the use of PDFs to represent subjective assessments of ranges for each of the parameters with median values shown in **Table 4**. We also assume a description of "thindown" at low energies, where the track width of a particle becomes smaller than the biological target. Here at low energies, the Risk cross section is modified by the factor, $P_E = 1 - \exp(-E/E_{TD})$ to account for thindown. The value of $E_{TD} = 0.2$ is based on experimental data for H and He. This factor has a very small impact for heavy ions since at low E they make a very small contribution to GCR or SPE exposures. The parameter κ is assumed to have distinct values for light and heavy ions (**Table 4**).

The cancer risk cross section or related quality factor is expressed in terms of the track structure parameter, $X_t = Z^2 / \beta^2$, using the Barkas form for the effective charge function. The quality factor

Table 4. Cancer Risk Cross Section or Quality factor parameters for solid cancer and leukemia risks*.

Parameter	Solid Cancer	Leukemia
m	3	3
κ	550 (1000)	550 (1000)
$\Sigma_0 / \alpha_\gamma, \mu m^2 Gy$	7000/6.24	1750/6.24
E_{TD}	0.2 MeV/u	0.2 MeV/u

*Values in parenthesis for when distinct values for light ions ($Z \leq 4$) are to be used.

has an additional dependence on LET, which relates the particle track structure to the absorbed dose (Cucinotta *et al.*, 2011). **Figure 2** compares the NASA quality factor to the ICRP model used at NASA in the past for p, C, Si, and Fe nuclei versus LET illustrating the differences as described. The preferred slope on the rising side with increasing ionization density of $m=3$ is different than the ICRP $Q(LET)$, which rises approximately as $m=2$.

For calculations for a specific particle described by Z and E , Eq. (2) is replaced by

$$(11) \quad \lambda_{ZI}(F_T, a_E, a) = \lambda_{\gamma j}(a_E, a) \left\{ D_T(E, Z)(1 - P(Z, E)) + (\Sigma_0 / \alpha_{\gamma}) P(Z, E) F_T(Z, E) \right\}$$

where $\lambda_{\gamma j}$ is the inner bracketed terms in Eq. (2) that contains the ERR and EAR functions for individual tissues. Using the HZETRN code or similar radiation transport codes, the fluence spectra, $F(X_{tr})$ can be found by transforming the energy spectra, $\phi_j(E)$ for each particle, j of mass number and charge number, A_j and Z_j respectively as:

$$(12) \quad F(X_{tr}) = \sum_j \left(\frac{\partial X_{tr}}{\partial E} \right)^{-1} \phi_j(E)$$

where we evaluate the Jacobian in Eq. (12) using the Barkas (1963) form for the effective charge number given by

$$(13) \quad Z^* = Z(1 - e^{-125\beta/Z^{2/3}})$$

The tissue specific cancer incidence rate for GCR or SPEs can then be written:

$$(14) \quad \lambda_{IT} \approx \lambda_{I\gamma} \left\{ \sum_j \int dE \phi_{jT}(E) S_j(E) (1 - P(X_{tr})) + (\Sigma_0 / \alpha_{\gamma}) \int dX_{tr} F(X_{tr}) P(X_{tr}) \right\}$$

The first term on the right hand side of Eq. (14) can be well approximated by the tissue averaged absorbed dose times the low LET risk coefficient. This approximation can be shown to lead to <10% over-estimation of its true value. However, in REIC calculations the error is even smaller because the second term of the right-hade side of Eq.(14) is dominant. We modified the HZETRN and BRYNTRN codes to perform the exact calculation, however for the Monte-Carlo uncertainty analysis described below, we use the following form for the radiation cancer rate for the mixed particle and energy fields in space:

$$(14') \quad \lambda_{IT} \approx \lambda_{I\gamma} \left\{ Dose + \Sigma_0 \left[\int dX_{tr} F_{LI}(X_{tr}) P_{LI}(X_{tr}) + \int dX_{tr} F_{HI}(X_{tr}) P_{HI}(X_{tr}) \right] \right\}$$

where we distinguish spectra for light ions ($Z \leq 4$), F_{LI} from heavy ions, F_{HI} ($Z > 4$). A summation over all cancer types is made for the radiation contribution to the survivor function in evaluating tissue specific risks, and a further summation over all cancer types to evaluate the over-all cancer risk.

In organ exposure evaluations, fluence spectra are averaged over each tissue using body shielding models. In **Figure 3** we show differential REIC spectra versus X_{tr} at solar minimum behind increasing amounts of aluminum shielding for a Mars and ISS mission. Calculations are made with the HZETRN code using the Badhwar and O'Neill GCR model (1992) and QMSFRG nuclear cross section data base (Cucinotta *et al.*, 2007). Results are shown on a linear-log plot

such that the area under the curve for each decade of X_{tr} is equally weighted. Leukemia risk shows a reduced maximum Q-value compared to solid cancer risks, resulting in particles at lower values of X_{tr} making larger contributions compared to solid cancer risks. **Figure 3** shows sharp spikes at increasing values of Z^2 for each GCR charge group. For example, at small values of X_{tr} we see peaks at 1 and 4, corresponding to protons and He nuclei. At large values of X_{tr} we observe a prominent peak near $Z^2/\beta^2 = 676$ corresponding to relativistic Fe nuclei. These sharp peaks correspond to the contributions from relativistic particles, with broader peaks for deep space exposure due to contribution of low to medium energy GCR not present in the ISS orbit due to the Earth's geomagnetic field.

In **Figure 4a** (Cucinotta *et al.*, 2011) we compare calculations of annual Effective dose in the ICRP model to the NASA recommended model for ISS missions at solar minimum and maximum. Comparisons for aluminum and polyethylene shielding are shown. **Figure 4b** shows similar comparisons for 1-year in deep space. The ICRP model provides higher estimates at shallow shielding depth due largely to its higher estimation of contributions for relativistic particles than the NASA model. At deep shielding depths, the NASA model gives higher estimates due to its assignment of higher biological effectiveness to low energy proton and helium nuclei produced by neutrons and other particles and from atomic slowing-down of primaries. For the various

Figure 2. Comparison of LET dependence for H, C, Si, and Fe nuclei in the proposed NASA Quality factors for solid cancer and leukemia risk estimation to quality factors from ICRP (ICRP, 1990).

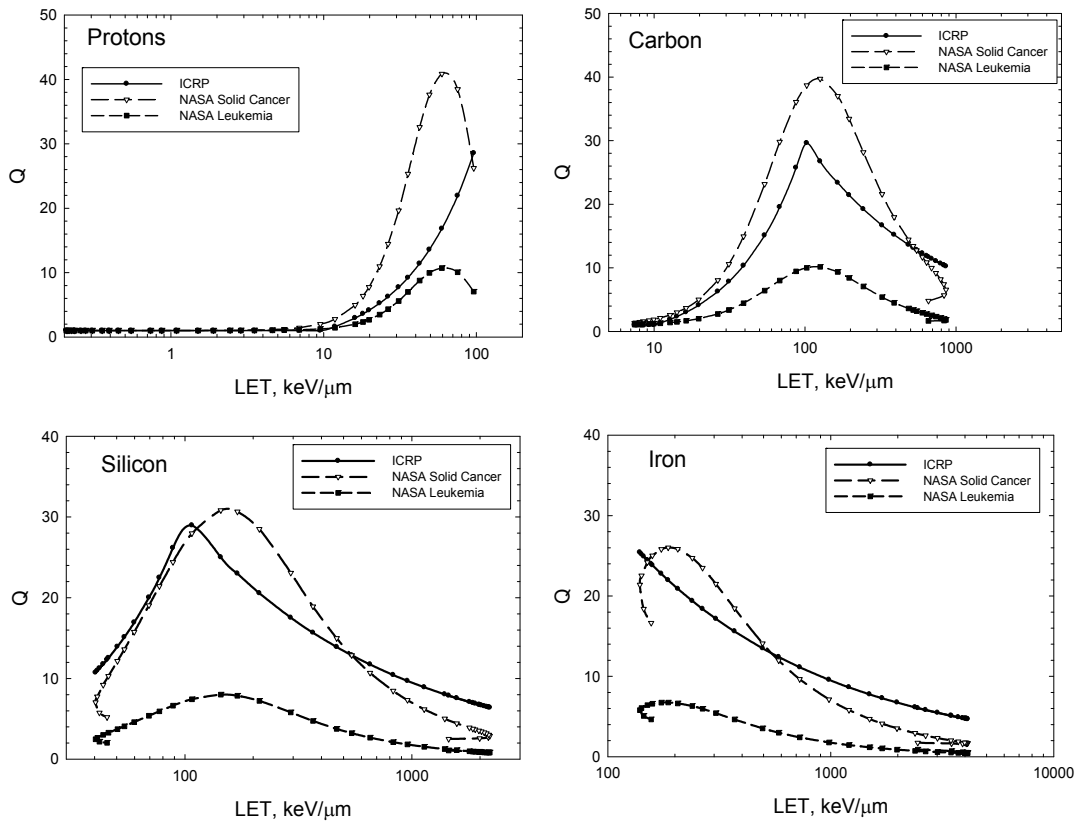


Figure 3a. Leukemia and solid cancer risk distribution for 40-y Females versus Z^{*2}/β^2 on 6 month ISS mission at solar minimum with 20 g/cm² of aluminum shielding .

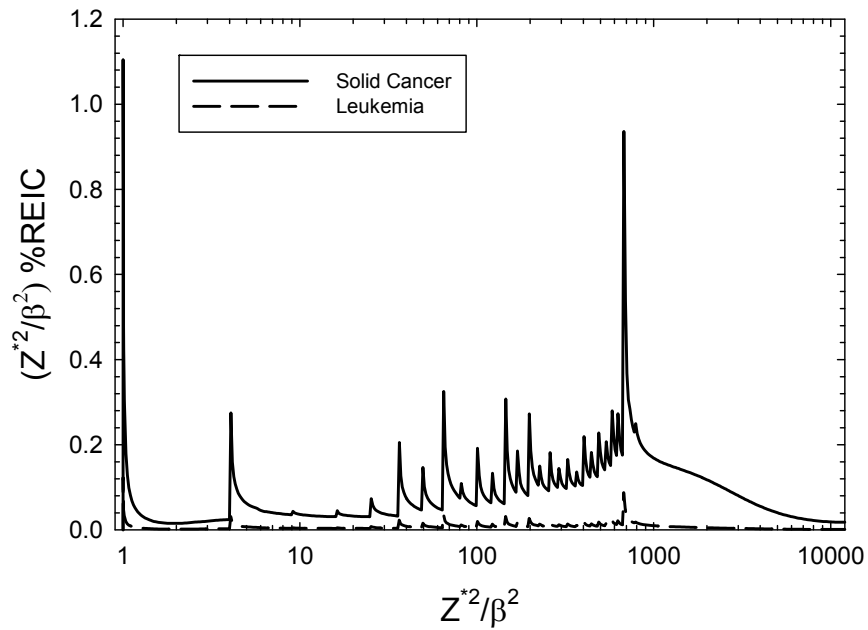


Figure 3b. Leukemia and solid cancer risk distribution for 40-y Females versus Z^{*2}/β^2 for 30 month Mars mission including 18 month surface stay at solar minimum with 20 g/cm² of aluminum shielding.

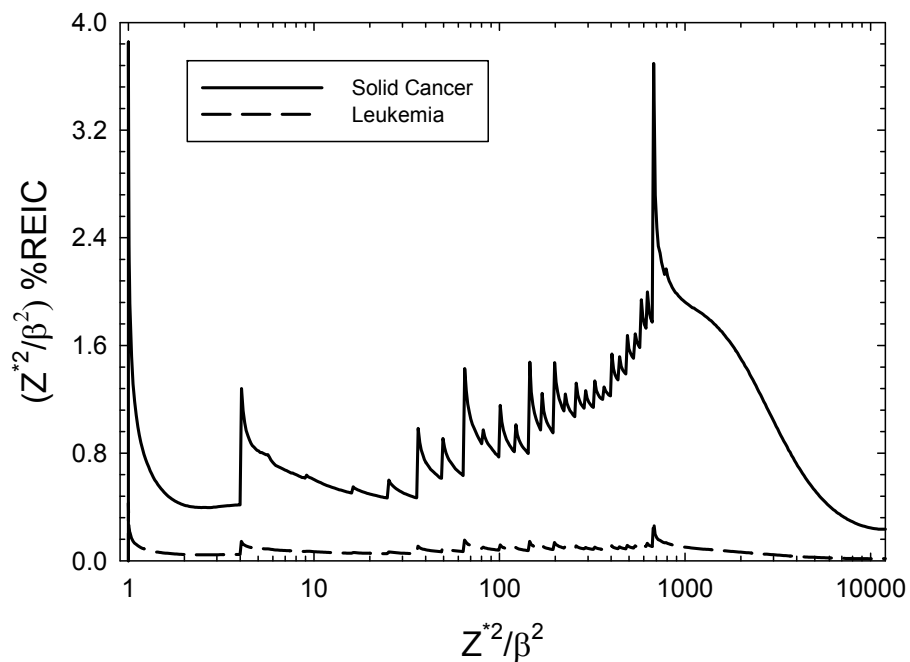


Figure 4a. Comparison of annual Effective dose for males in ISS orbit (51.6 deg x 400 km) versus depth of shielding. Values for solar min and maximum are shown comparing ICRP model to recommended NASA model.

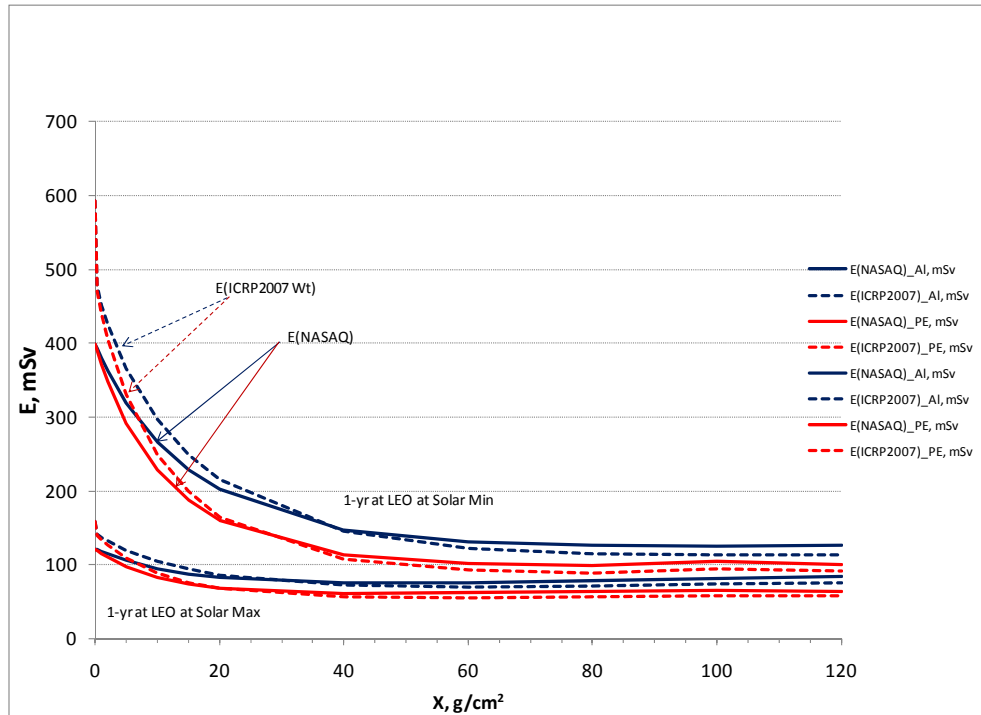
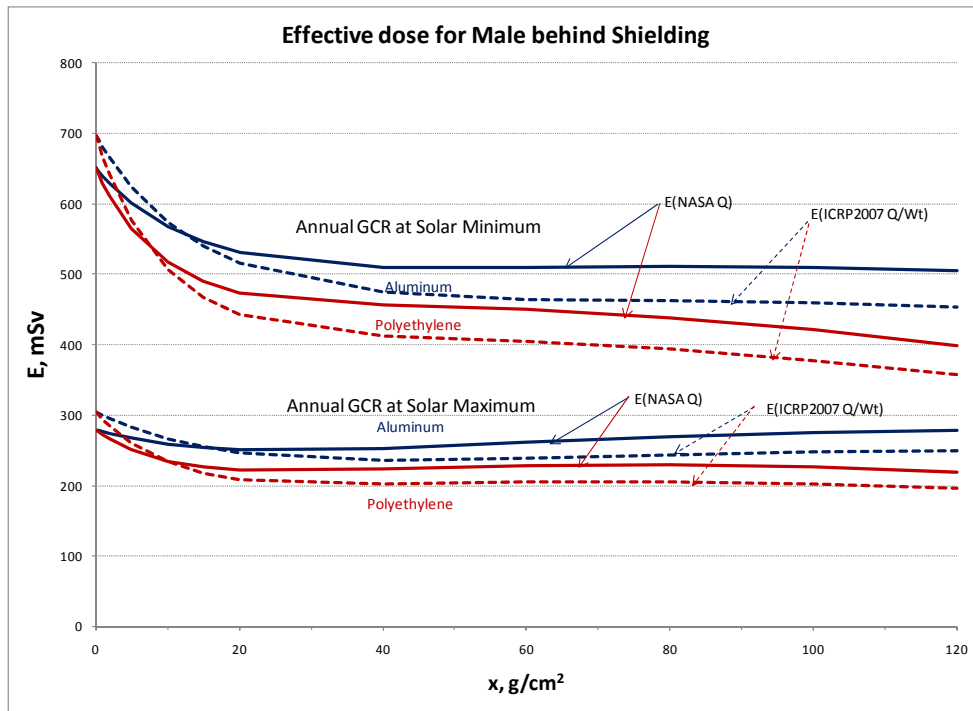


Figure 4b. Annual GCR Effective doses in deep space versus depth of shielding for males. Values for solar min and maximum are shown comparing ICRP model to recommended NASA model.



mission and shielding scenarios, differences in Effective doses are on the order of 10 to 30%, however the NASA model allows for an improved uncertainty assessment to be made than the ICRP Q function whose parameters are difficult to relate to biophysical interpretation. Of note is that shielding only provides a minor reduction in GCR organ dose equivalent. Most of the reduction occurs in the first 20 g/cm² of material at solar minimum. The reduced number of low energy particles at solar maximum reduces even this benefit from shielding. To significantly reduce GCR beyond this initial reduction would require several meters of hydro-carbon shielding.

4. Uncertainty Analysis

To propagate uncertainties across multiple contributors we performed Monte-Carlo simulations sampling over subjective probability distribution functions (PDF) that represent current knowledge of factors that enter into risk models (NCRP, 1997; 2006; Cucinotta *et al.*, 2001, 2006; 2011). In a simplified manner, we can write a risk equation as a product of several factors including the dose, D , quality factor, Q , a low LET risk coefficient normally derived from the data of the atomic-bomb survivors, R_0 , and the dose and dose-rate reduction effectiveness factor, $DDREF$, that corrects risk data for dose-rate modifiers. Monte-Carlo uncertainty analysis uses the risk equation, but modified by normal deviates that represent subjective weights and ranges of values for various factors that enter into a risk calculation. First, we define $X \in R(x)$ as a random variate that takes on quantiles x_1, x_2, \dots, x_n such that $p(x_i) = P(X=x_i)$ with the normalization condition $\sum p(x_i)=1$. $C(x_i)$ is defined as the cumulative distribution function, $C(x)$, which maps X into the uniform distribution $U(0, 1)$ and we define the inverse cumulative distribution function $C(x)^{-1}$ in order to perform the inverse mapping of $U(0, 1)$ into x : $x=C(x)^{-1}$. Then we write for a simplified form of the risk equation for a Monte-Carlo trial, ξ :

$$(15) \quad Risk_{\xi} = R_0(\text{age, gender}) \frac{FLQ}{DDREF} \left\{ \frac{x_{R_0} x_{phys} x_Q}{x_{D_R}} \right\}_{\xi}$$

where R_0 is the low LET risk coefficient per unit dose, the absorbed dose, D is written as the product of the particle fluence, F and LET, L , and Q the radiation quality factor. The x_{R_0} , x_{phys} , x_{D_R} , and x_Q are quantiles that represent the uncertainties in the low LET risk coefficient, the space physics models of organ exposures, dose-rate effects, and radiation quality effects, respectively. Monte-Carlo trials are repeated many times, and resulting values binned to form an overall probability distribution function (PDF) taken into account each of the model uncertainties. In practice, the risk model does not use the simple form of Eq.(15). Instead risk calculations are made using the REIC described by Eq. (1). For the 95% Confidence intervals for the %PC, we use the bootstrap method to infer the values from the uncertainty analysis for REIC.

PDF functions describing the uncertainties to the quantiles, x_{ξ} for the various parameters in the model are described in **Table 5** from the recent report by Cucinotta *et al.* (2011). Two modifications are to introduce tissue specific statistical uncertainties and to include uncertainties in the estimate of RR for NS compared to the U.S. average. The subjective PDF's are then employed in the Monte-Carlo calculation to describe a given space radiation scenario as described previously (Cucinotta *et al.*, 2001; 2006; 2011). The point estimate for Q_{max} of 40, occurs for the most effective proton energy (~ 0.5 MeV). Values assigned give more weight to the animal model solid tumor data and are influenced by fractionation studies that

Table 5. Summary of PDF for Uncertainty Components in NASA Model.

Uncertainty Contribution	PDF form for Quantile, x_i	Comment
<u>Low LET Model:</u>		
Statistical Errors	See Table 6	Tissue specific values used
Statistical Errors in RR for Never-smokers	Normal (M=1.0; SD=0.25)	Applied to tissues considered in Table 3 for NS
Bias in Incidence data	Normal (M=1.0; SD = 0.05)	Based on NCRP Report 126
Dosimetry Errors	Log-Normal (GM=0.9, GSD=1.3)	Based on Preston <i>et al.</i> (2007); UNSCEAR (2008)
Transfer model weights	Uniform distribution about preferred weight	Ignored for breast and thyroid cancers
DDREF	Log-Normal (GM=1.0; GSD=1.4)	DDREF=1.75; Truncated at 0.75 for inverse dose-rate probability <0.05
<u>Risk Cross Section or Q:</u>		
Σ_0/α_γ	Log-normal(GM=0.9; GSD=1.4)	GM<1 assumes existing data is biased to higher values
κ	Normal(M=1, SD=0.2)	Position of peak estimates suggests variation on sensitivity, target size/ distributed targets
m	Discrete $m=[1.5,2,2.5,3,3.5,4]$ with weights [.05,.1,.2,.4,.2,..05]	Values restricted over (1.5,4)
<u>Physics Uncertainties:</u>		
$F(Z^2/\beta^2)$ for $Z<5$	Normal (M=1.05; SD=1/3)	HZETRN does not account for mesons, e- and γ -rays that are low Charge and high velocity; may underestimate neutron recoils of low charge
$F(Z^2/\beta^2)$ for $Z\geq 5$	Normal (M=1.0; SD=1/4)	HZETRN accurate at high Z

suggest that higher RBE's are possible. The resulting PDF has a 95% C.I. for the maximum value of Q for solid cancer as [14, 70], which covers most of the range of values from Fe nuclei tumor induction and earlier neutron studies reflective of low energy protons. In **Table 4** we use a GM=0.9 for the PDF associated with Σ_0/α_γ with the expectation that some tissues would have lower values as found for leukemia; however there is a lack of information to make a more informed choice. In an alternative model of the radiation quality uncertainties, we assume that the slope, m is correlated with the position of the maximum value of Q as determined by the value of κ . After studying the functional dependence of the parameters of Eq. (10), we find the position of the maximum Q is held fixed for differential values of m if we use the constraint:

$$(16) \quad \kappa(m) = \frac{4\kappa_0}{(m+1)}$$

where κ_0 is the estimated value from **Table 4**. This alternative uncertainty assessment assumes that the kinetic energy for each Z at the maximum of the risk cross section for cancer induction in humans is fairly well described by the existing data. In this approach uncertainties in the maximum Q value, slope of Q with changing X_{tr} , and kinetic energy at the Q maximum are described, however these values are more constrained compared to the uncertainty analysis without this constraint. The alternative uncertainty model was applied using conditional Monte-

Carlo sampling, where a random value of m is selected from its PDF, prior to sampling for the κ value with central estimate defined by Eq.(16).

Statistical Uncertainties for Tissue Specific Estimates

For estimating the statistical uncertainties for overall cancer risks from radiation we previously used (Cucinotta *et al.*, 2011) the recommendations from NCRP Report 126 (1997) for the statistical uncertainty in the total cancer risk derived from cancer mortality data of the LSS survivors. However, larger statistical uncertainties occur for tissue specific risk estimates derived from cancer incidence data. The various reports on tissue specific estimates of cancer risks (BEIR VII, 2006; UNSCEAR 2008; Preston *et al.*, 2007) typically combine statistical uncertainties with dosimetry or other uncertainties in reporting confidence levels. The UNSCEAR report did not report uncertainty ranges for their model EAR and ERR functions, which further complicates assessments of tissue specific statistical uncertainties. The approach used here is to introduce subjective PDF's for the tissue specific statistical uncertainties based on the Empirical Bayes (EB) results from Pawel *et al.* (2009). The important feature of the EB approach is to consider the correlation between the standards errors for different tissue sites **Table 6** shows results from this work. In the last two

Table 6. Comparison of Maximum likelihood estimates (MLE) to Empirical Bayes (EB) method for gender adjusted site-specific ERR from the LSS study (Pawel *et al.* 2008), and %SD estimates and Subjective %SD estimates used for model calculations in parenthesis.

<i>Tissue</i>	<i>ERR/Sv Estimate</i>		<i>Standard Error</i>		<i>%SD EB (subjective)</i>
	<i>MLE</i>	<i>EB</i>	<i>MLE</i>	<i>EB</i>	
Stomach	0.32	0.32	0.06	0.06	0.19 (0.2)
Colon	0.49	0.47	0.11	0.10	0.21 (0.2)
Liver	0.31	0.32	0.10	0.09	0.28 (0.3)
Lung	0.70	0.63	0.13	0.11	0.18 (0.2)
Breast	0.67	0.63	0.10	0.09	0.14 (0.25)
Prostate	0.18	0.32	0.30	0.19	0.60 (0.6)
Uterus	0.04	0.05	0.05	0.05	1.0 (1.0)
Ovary	0.27	0.32	0.19	0.15	0.47 (0.5)
Bladder	0.84	0.58	0.29	0.18	0.31 (0.3)
Esophagus	0.63	0.48	0.31	0.19	0.40 (0.4)
CNS	0.37	0.38	0.17	0.14	0.37 (0.4)
Thyroid					(0.4)
Oral Cavity	0.34	0.36	0.15	0.13	0.36 (0.4)
Remainder*	1.15	0.85	0.19	0.15	0.18 (0.2)
Leukemia					(0.25)

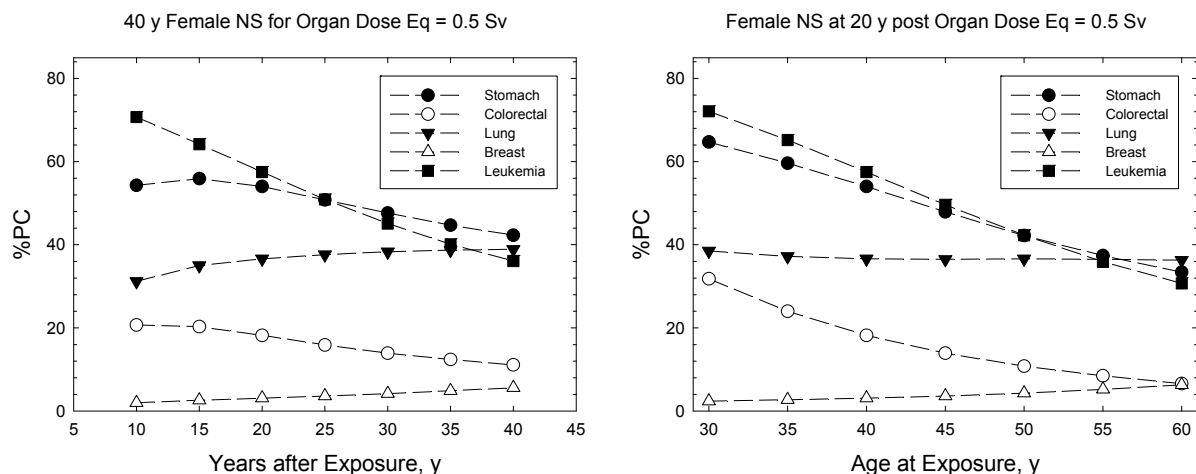
*Remainder included different tissues in various reports described in Text.

columns we show results as the %SD relative to the mean estimate, and the subjective values used in our analysis are shown in parenthesis. Note that statistical errors for leukemia were not considered by Pawel et al. (2009) and for thyroid and breast cancers, meta-analysis results that included data in addition to the Japanese atomic-bomb survivor data was considered as recommended by BEIR VII (2006).

5. RESULTS

Figure 5 illustrates some general characteristics of the %PC for different tissue sites. Calculations are shown for an organ dose equivalent of 0.5 Sv to each tissue site for a Female NS. Results for leukemia are made at the same the organ dose equivalent as solid cancers, however the NASA model would assign a smaller Q-factor for leukemia resulting in a smaller GCR organ dose equivalent for the bone marrow compared to values for solid tissues. The left panel of **Fig. 5** shows calculation for an age of exposure of 40 y and the dependency of the %PC with time after exposure. Different trends occur for the tissues shown, which are largely determined by the age and time after exposure dependences of the fitted EAR and ERR functions, and the age dependence of the background rates for the tissues. Similar trends are observed for males (data not shown) The %PC peaks early after exposure for leukemia and stomach cancers and rises slowly with time after exposure for breast and lung cancers. There are additional uncertainties that are not accounted for with regards to the calculation of %PC less than 2 and 5 years after exposure for leukemia and solid cancer, respectively because epidemiology data is often sparse at these times. In addition heavy ion and neutrons appear to cause an earlier induction of cancers than low LET radiation, which is not accounted for in the current models of cancer risk (NCRP 2000; NCRP 2006). In right panel of **Fig. 5** we show calculations of %PC at 20 years post-exposure for different ages of exposure. The %PC declines with age at exposure for most but not all tissues because background cancer risks tend to increase with age.

Figure 5. Calculations of %PC for NS Females for organ dose equivalents of 0.5 Sv. The left panel shows results versus time after exposure and the right panel versus age at exposure for disease diagnosis at 20 y post-exposure.



In **Tables 7, 8 and 9** we show estimates of tissue specific %REIC and 95% CL, and point estimates and upper 95% CL for %PC for a 1-year NEA mission, a 30 month Mars mission, and a 6-month ISS mission, respectively. Calculations for males and females represented by the U.S. average population or a population of NS are shown. For %PC estimates results are shown for disease diagnosis at 20 year post exposure. Results are based on the UNSCEAR (2007) models for many tissues with the exceptions for noted before for breast, thyroid, and prostate cancer (Cucinotta *et al.*, 2011). Similar results would be found using the BEIR VII models, however the BEIR VII model did not include an age at exposure dependence for rates above age 30 y (BEIR VII), and therefore the NASA 2010 model used the UNSCEAR models for EAR and ERR rate functions. All results are for solar minimum conditions assuming 20 g/cm² aluminum shielding. However, **Figure 4** shows that larger amounts of shielding (up to 120 g/cm²) would not change the results significantly, and a modest improvement is made by using polyethylene or water equivalent shielding compared to aluminum. Any time spent on extra-vehicular activities (EVA) would marginally increase these results for solar minimum conditions. At solar maximum, the uncertainty in solar particle event (SPE) environments is an important consideration (Kim *et al.*, 2009). SPE's uncertainties related to time of occurrence, total fluence and energy spectra play a much larger role for EVA's and will be considered elsewhere.

The estimates of PC for stomach and leukemia cancers show the largest association with GCR exposures followed by colon, liver, bladder, and lung cancers. An important gender dependence occurs between values for several tissues. For a Mars mission, estimates of the %PC at the 95% confidence level would suggest a large proportion of cancers that would be observed in astronauts would be either caused or moved forward in time by radiation exposure. In contrast, a single ISS mission at solar minimum does not lead to %PC estimates above 50% for any tissue even at the 95% CL. However, for an individual making two or more ISS missions, PC values for leukemia and stomach cancers would likely exceed 50% at the 95% CL, and lung cancer PC estimates for NS would approach 50% at the 95% CL. The results shown in **Table 8** are for the conjunction type Mars mission. In comparison the shorter opposition class missions have more time in deep space than the conjunction class missions. Thus the conjunction class missions, which have long stays on the Mars surface, benefit from the 2π shielding provided by the solid body of Mars and its atmospheric shielding. The net effect is for a decreased risk for conjunction class missions compared to opposition class missions at solar minimum. The same is true at solar maximum because the risk of a high SPE exposure on the Mars surface is greatly reduced compared to the SPE risk in deep space.

Table 7a. Lifetime %REIC and 95% CI, and %PC for 60 y Females following 1-year NEA mission at age 40 y. Calculations assume 20 g/cm² aluminum shielding for solar minimum conditions.

<i>Tissue</i>	<i>%REIC</i>	<i>%PC</i> (95% CL)	<i>%REIC</i>	<i>%PC</i> (95% CL)
	<i>U.S. Ave. Females</i>		<i>NS Females</i>	
Stomach	0.331 [0.091, 1.31]	54.0 (82.2)	0.347 [0.095, 1.39]	57.6 (84.5)
Colon	0.461 [0.135, 1.79]	21.1 (51.0)	0.439 [0.128, 1.71]	21.2 (51.1)
Liver	0.117 [0.026, 0.459]	27.7 (60.0)	0.117 [0.026, 0.466]	34.6 (67.9)
Lung	2.06 [0.602, 8.02]	21.6 (51.7)	0.815 [0.238, 3.20]	41.2 (73.3)
Breast	0.737 [0.215, 2.88]	5.98 (19.9)	0.779 [0.228, 3.00]	5.99 (20.1)
Uterus	0.133 [0.008, 0.791]	5.73 (26.6)	0.140 [0.009, 0.835]	5.74 (26.6)
Ovary	0.156 [0.018, 0.693]	11.7 (37.1)	0.165 [0.019, 0.742]	11.7 (37.3)
Bladder	0.331 [0.079, 1.29]	19.0 (47.6)	0.299 [0.071, 1.18]	22.1 (53.0)
Esophagus	0.034 [0.006, 0.141]	15.7 (43.5)	0.016 [0.003, 0.069]	23.8 (56.7)
Brain-CNS	0.044 [0.007, 0.183]	12.1 (36.5)	0.046 [0.007, 0.194]	12.1 (36.7)
Thyroid	0.123 [0.021, 0.516]	12.1 (36.6)	0.126 [0.021, 0.531]	12.1 (36.7)
Oral Cavity	0.022 [0.004, 0.090]	5.70 (20.1)	0.022 [0.004, 0.094]	11.6 (35.5)
Remainder	0.479 [0.132, 1.90]	-	0.242 [0.066, 0.958]	-
Leukemia	0.392 [0.142, 1.38]	57.3 (82.5)	0.344 [0.125, 1.22]	62.2 (85.5)
Total	5.71 [1.77, 20.8]	-	4.11 [1.35, 15.1]	-

Table 7b. Lifetime %REIC and 95% CI, and %PC for 60 y Males following 1-year NEA mission at age 40 y. Calculations assume 20 g/cm² aluminum shielding for solar minimum conditions.

<i>Tissue</i>	<i>%REIC</i>	<i>%PC</i> (95% CL)	<i>%REIC</i>	<i>%PC</i> (95% CL)
	<i>U.S. Ave. Males</i>		<i>NS Males</i>	
Stomach	0.316 [0.087, 1.23]	38.7 (71.0)	0.329 [0.085, 1.29]	45.8 (76.7)
Colon	0.491 [0.135, 1.89]	20.8 (50.3)	0.485 [0.133, 1.87]	20.8 (50.3)
Liver	0.141 [0.031, 0.549]	12.3 (35.3)	0.131 [0.029, 0.513]	14.9 (40.8)
Lung	0.750 [0.206, 2.88]	6.87 (22.1)	0.386 [0.106, 1.50]	30.1 (62.6)
Prostate	0.289 [0.023, 1.38]	1.94 (8.63)	0.319 [0.025, 1.53]	1.94 (8.66)
Bladder	0.677 [0.150, 2.61]	14.6 (39.7)	0.466 [0.103, 1.82]	16.7 (43.9)
Esophagus	0.109 [0.016, 0.45]	11.4 (34.7)	0.037 [0.006, 0.151]	14.0 (40.1)
Brain-CNS	0.045 [0.007, 0.186]	9.40 (30.0)	0.049 [0.007, 0.201]	9.41 (30.1)
Thyroid	0.024 [0.004, 0.1]	6.26 (21.5)	0.026 [0.004, 0.107]	6.27 (21.5)
Oral Cavity	0.019 [0.004, 0.076]	1.83 (6.94)	0.020 [0.004, 0.082]	7.32 (24.6)
Remainder	0.419 [0.108, 1.65]	-	0.198 [0.051, 0.771]	-
Leukemia	0.612 [0.211, 2.13]	59.9 (83.4)	0.537 [0.186, 1.89]	66.1 (87.3)
Total	4.00 [1.31, 14.6]	-	3.07 [1.01, 11.2]	-

Table 8a. Lifetime %REIC and 95% CI, and %PC for 60 y Females following 30 month Mars mission at age 40 y. Calculations assume 20 g/cm² aluminum shielding for solar minimum conditions.

<i>Tissue</i>	<i>%REIC</i>	<i>%PC</i> (95% CL)	<i>%REIC</i>	<i>%PC</i> (95% CL)
	<i>U.S. Ave. Females</i>		<i>NS Females</i>	
Stomach	0.556 [0.153, 2.15]	66.8 (88.6)	0.585 [0.161, 2.31]	70.0 (90.2)
Colon	0.762 [0.223, 2.91]	31.3 (63.5)	0.728 [0.213, 2.82]	31.4 (63.9)
Liver	0.198 [0.044, 0.769]	39.7 (71.9)	0.198 [0.044, 0.792]	47.7 (78.5)
Lung	3.46 [1.010, 12.5]	31.9 (63.7)	1.37 [0.401, 5.22]	54.3 (81.9)
Breast	1.18 [0.345, 4.44]	9.65 (28.7)	1.25 [0.366, 4.83]	9.67 (29.2)
Uterus	0.223 [0.014, 1.32]	9.43 (38.1)	0.235 [0.015, 1.39]	9.45 (38.2)
Ovary	0.261 [0.030, 1.13]	18.5 (49.7)	0.278 [0.032, 1.22]	18.5 (49.9)
Bladder	0.559 [0.134, 2.07]	28.7 (59.8)	0.508 [0.122, 1.93]	32.8 (65.0)
Esophagus	0.057 [0.010, 0.234]	24.1 (56.4)	0.028 [0.005, 0.113]	34.8 (68.6)
Brain-CNS	0.072 [0.012, 0.294]	18.8 (48.6)	0.076 [0.013, 0.314]	18.9 (49.0)
Thyroid	0.187 [0.032, 0.788]	18.7 (49.1)	0.194 [0.033, 0.818]	18.7 (49.3)
Oral Cavity	0.035 [0.007, 0.143]	9.14 (29.0)	0.037 [0.007, 0.152]	17.9 (47.5)
Remainder	0.777 [0.213, 2.95]	-	0.394 [0.108, 1.52]	-
Leukemia	0.651 [0.236, 2.24]	69.5 (88.7)	0.573 [0.208, 2.0]	73.6 (90.7)
Total	9.41 [3.09, 33.1]	-	6.78 [2.22, 24.3]	-

Table 8b. Lifetime %REIC and 95% CI, and %PC for 60 y Males following 30 month Mars mission at age 40 y. Calculations assume 20 g/cm² aluminum shielding for solar minimum conditions.

<i>Tissue</i>	<i>%REIC</i>	<i>%PC</i> (95% CL)	<i>%REIC</i>	<i>%PC</i> (95% CL)
	<i>U.S. Ave. Males</i>		<i>NS Males</i>	
Stomach	0.530 [0.145, 2.05]	52.1 (80.8)	0.555 [0.152, 2.18]	59.2 (85.1)
Colon	0.816 [0.238, 3.14]	30.9 (63.3)	0.807 [0.221, 3.11]	31.0 (63.3)
Liver	0.237 [0.053, 0.918]	19.4 (48.2)	0.221 [0.049, 0.87]	23.1 (54.3)
Lung	1.26 [0.369, 4.71]	11.2 (32.0)	0.652 [0.179, 2.47]	42.4 (73.6)
Prostate	0.483 [0.047, 2.27]	3.25 (13.6)	0.535 [0.052, 2.53]	3.25 (13.7)
Bladder	1.15 [0.254, 4.34]	22.7 (52.7)	0.792 [0.175, 3.01]	25.6 (56.7)
Esophagus	0.184 [0.031, 0.749]	18.1 (47.3)	0.062 [0.009, 0.252]	21.8 (53.1)
Brain-CNS	0.073 [0.012, 0.298]	14.9 (41.6)	0.080 [0.013, 0.326]	14.9 (41.8)
Thyroid	0.038 [0.006, 0.157]	10.2 (32.0)	0.041 [0.007, 0.170]	10.2 (32.0)
Oral Cavity	0.031 [0.006, 0.122]	3.03 (11.1)	0.032 [0.006, 0.132]	11.8 (35.3)
Remainder	0.683 [0.188, 2.60]	-	0.325 [0.089, 1.23]	-
Leukemia	1.02 [0.351, 3.50]	71.8 (89.8)	0.891 [0.308, 3.09]	76.9 (92.0)
Total	6.70 [2.20, 23.6]	-	5.15 [1.69, 18.3]	-

Table 9a. Lifetime %REIC and 95% CI, and %PC for 60 y females following ISS mission at age 40 y. Calculations assume 20 g/cm² aluminum shielding for solar minimum conditions with mission length of 180 d.

<i>Tissue</i>	<i>%REIC</i>	<i>%PC</i> (95% CL)	<i>%REIC</i>	<i>%PC</i> (95% CL)
	<i>U.S. Ave. Females</i>		<i>NS Females</i>	
Stomach	0.031 [0.008, 0.126]	9.75 (30.4)	0.032 [0.008, 0.131]	11.1 (33.7)
Colon	0.043 [0.012, 0.172]	2.38 (8.88)	0.041 [0.011, 0.161]	2.39 (8.82)
Liver	0.011 [0.002, 0.045]	3.41 (12.6)	0.011 [0.002, 0.044]	4.67 (16.6)
Lung	0.192 [0.053, 0.765]	2.45 (9.10)	0.075 [0.021, 0.304]	5.99 (20.4)
Breast	0.069 [0.019, 0.276]	0.57 (2.24)	0.072 [0.020, 0.291]	0.57 (2.26)
Uterus	0.012 [0.0, 0.075]	0.56 (3.26)	0.013 [0.0, 0.078]	0.56 (3.26)
Ovary	0.015 [0.002, 0.066]	1.20 (5.25)	0.015 [0.002, 0.070]	1.20 (5.27)
Bladder	0.031 [0.007, 0.126]	2.12 (8.02)	0.028 [0.006, 0.113]	2.56 (9.57)
Esophagus	0.003 [0.001, 0.014]	1.68 (6.79)	0.002 [0.000, 0.006]	2.78 (10.8)
Brain-CNS	0.004 [0.001, 0.017]	1.22 (5.01)	0.004 [0.001, 0.018]	1.22 (5.01)
Thyroid	0.011 [0.002, 0.048]	1.21 (4.95)	0.012 [0.002, 0.049]	1.21 (4.93)
Oral Cavity	0.002 [0.001, 0.009]	0.59 (2.21)	0.002 [0.001, 0.009]	1.21 (4.68)
Remainder	0.045 [0.012, 0.180]	-	0.022 [0.006, 0.091]	-
Leukemia	0.036 [0.012, 0.129]	10.9 (30.4)	0.031 [0.011, 0.113]	13.0 (35.0)
Total	0.529 [0.164, 1.99]	-	0.379 [0.117, 1.43]	-

Table 9b. Lifetime %REIC and 95% CI, and %PC for 60 y males following ISS mission at age 40 y. Calculations assume 20 g/cm² aluminum shielding for solar minimum conditions with mission length of 180 d.

<i>Tissue</i>	<i>%REIC</i>	<i>%PC</i> (95% CL)	<i>%REIC</i>	<i>%PC</i> (95% CL)
	<i>U.S. Ave. Males</i>		<i>NS Males</i>	
Stomach	0.029 [0.008, 0.117]	5.52 (18.9)	0.031 [0.008, 0.122]	7.25 (23.7)
Colon	0.045 [0.012, 0.179]	2.34 (8.64)	0.045 [0.012, 0.174]	2.35 (8.54)
Liver	0.013 [0.003, 0.053]	1.28 (4.91)	0.012 [0.003, 0.049]	1.59 (6.08)
Lung	0.070 [0.019, 0.274]	0.67 (2.59)	0.036 [0.010, 0.142]	3.80 (13.5)
Prostate	0.027 [0.002, 0.130]	0.18 (0.87)	0.029 [0.002, 0.143]	0.18 (0.87)
Bladder	0.064 [0.014, 0.252]	1.56 (5.91)	0.044 [0.010, 0.173]	1.82 (6.87)
Esophagus	0.010 [0.002, 0.043]	1.18 (4.77)	0.003 [0.001, 0.014]	1.47 (5.87)
Brain-CNS	0.004 [0.001, 0.017]	0.93 (3.79)	0.004 [0.001, 0.019]	0.93 (3.78)
Thyroid	0.002 [0.000, 0.010]	0.61 (2.48)	0.002 [0.000, 0.010]	0.61 (2.46)
Oral Cavity	0.003 [0.001, 0.008]	0.23 (0.71)	0.002 [0.001, 0.008]	0.77 (2.92)
Remainder	0.039 [0.010, 0.155]	-	0.018 [0.005, 0.073]	-
Leukemia	0.056 [0.019, 0.198]	12.0 (32.7)	0.049 [0.017, 0.175]	15.1 (38.9)
Total	0.372 [0.122, 1.38]	-	0.284 [0.093, 1.05]	-

6. Discussion and Conclusions

The results reported here suggest that a large portion of cancers that would be observed in crews after long-term missions to Near Earth Asteroids or Mars could be attributed to GCR exposure. However, it should be noted that current estimates of 95% confidence levels for the 3% REID limit would restrict deep space missions to 4 to 8 months depending on age, gender, and prior exposures. For example 40-y NS males and females with small prior exposures would be limited to 7- and 8-months, respectively with heavy shielding at solar minimum. Thus the %PC at the maximum allowed mission length would be reduced by about 30% from the values in **Table 7** for a NEA mission near solar minimum. In contrast, PC estimates for ISS missions are not estimated to be significant due to the smaller mission length and because of the larger fraction of crew exposures from the higher energy GCR and trapped protons, which have smaller quality factors and uncertainties compared to the full GCR spectrum in deep space. The deep space GCR environment contains a larger fraction of particles with kinetics energies below 1000 MeV/u than the ISS orbit, and HZE nuclei at these energies are expected to have the maximum biological effectiveness (Cucinotta *et al.*, 2011).

The majority of astronauts are surely classified as “healthy workers” based on established evidence of optimal nutrition, exercise, medical care, and never-smoker status reducing cancer risks. This leads to the paradoxical result that radiation cancer risks are estimated to be significantly reduced for NS and healthy workers such as astronauts compared to the average U.S. population, while probability of causation estimates for several cancer types are increased. Furthermore, the use of a NS population to represent astronauts may lead to an under-estimation of PC's, which is suggested by Kaplan-Meier survival analysis and SMR results of **Figure 1** and **Table 1**. These results suggest that adjustment for smoking effects does not account for the entire increase in longevity or reduced SMR found for astronauts at this time. Because multiplicative risk transfer models are most often used for solid cancer risk estimates, further research on categorizing healthy worker effects could play a significant role in both radiation risk and probability of causation estimates. In fact, the level of risk reduction predicted for NS's compared to the average U.S. population is greater than the organ dose equivalent reduction that would be provided to crew by more than 1-meter of polyethylene or water shielding. This suggests that research into healthy workers effects could lead to substantial cost reduction for a NEA or Mars missions, because of the very large cost to launch shielding into deep space in comparison to the costs of research efforts. Research into uncertainty reduction remains the principle approach to improvements in this and other areas of radiation risk estimation and mitigation.

Probability of causation provides an indicator of possible association, however clearly other information should be collected to ascertain potential causal relationships. A %PC above 50% either at the point estimate or at the 95% or even 99% CL has been used in compensation of workers including military and nuclear reactor workers (DHHS 2002; NIH 2003; Leigh and Wakeford, 2001). Family history and an individual's possible exposure to other carcinogens should be considered in an assessment of possible causality. The use of family history data should consider the possibility that genetic pre-disposition of specific cancer types (NCRP 2011) may also confer increased radiation sensitivity. Other factors to be considered include smoking history which effects lung, esophagus, oral, bladder and several other cancers, and reproductive history which can impact the risk of breast and other cancers in women (NIH 2003).

Stomach cancer and leukemia have the largest PC values, and astronauts that participate in two or more ISS missions could reach a significant PC for these tumor types. Our estimates used the NASA 2010 model, which assigns a smaller quality factors for leukemia compared to solid cancers. An even higher PC for leukemia would be predicted if the ICRP-60 quality factors were assumed. For stomach cancer risk estimates, we used the BEIR VII (2006) recommendation for tissue weighting factors for the relative contributions for multiplicative and additive risk transfer for stomach cancer. It is known that the use of the additive risk transfer model based on the Japanese A-bomb survivor data leads to a much higher risk estimate for stomach cancers in the U.S. population (NCRP, 1997) than the multiplicative transfer model. Studies of solid tumor risks across different strains of mice are supportive of multiplicative risk transfer (Storer *et al.*, 1988). The BEIR VII report (2006) recommended higher transfer weights for multiplicative risk transfer than earlier reports. This is a good example of the importance of improving the understanding of the extrapolation of radiation data between populations and from experimental results to humans because the choice of transfer models can widely change REIC and PC estimates for exploration missions.

The discovery of biomarkers of radiation induced cancers is an outstanding problem. Studies of cytogenetic signatures of thyroid cancer were reported (Nikiforov *et al.*, 1997), but very little information is available for other tissues. In recent years, molecular signatures of radiation causality have been investigated, including transcriptome analysis (Detours *et al.*, 2005; Port *et al.*, 2007; Ugolin *et al.*, 2011), however have led to conflicting results. For space radiation exposures research into biomarkers of causality is more challenging because of the types of radiation in space and lack of any human data. Approaches based on experimentally produced tumors in animal models should be considered, and will require improved understanding of methods of extrapolation to humans.

In future work, the approach used here will be extended to include other cancer types including non-melanoma skin cancer (Kim *et al.*, 2006), bone cancer, and components of the remainder term which includes renal, gallbladder, pancreatic, larynx, and several other cancers. Also, information of the components of leukemia and lung cancer risks should be considered and may allow for PC estimates based on distinct histological types for these tumors. In addition, more extensive Monte-Carlo evaluations should be made to report 99% confidence intervals, which are used in screening terrestrial radiation workers for possible compensation considerations. Reduction in the uncertainties in projecting space radiation risks through further cost-effective research will have the largest impact on these challenges to NASA and space exploration. Finally, it should be noted that NASA policy to limit REID to 3% at the 95% CL strongly overlaps with a goal of ensuring estimates of the PC for most cancer types do not reach a level of significance.

7. References

Badhwar GD, O'Neill PM. An improved model of GCR for space exploration missions. *Nucl. Tracks Radiat. Meas.* 20: 403-410; 1992.

Barkas H. *Nuclear Research Emulsions*. Academic Press Inc., New York. Vol. 1, Chap. 9, p. 371, 1963.

BEIR VII, National Academy of Sciences Committee on the Biological Effects of Radiation, Health Risks From Exposure to Low Levels of Ionizing Radiation. Washington DC: National Academy of Sciences Press; 2006.

Calle EE, Thun MJ, Petrelli JM, Rodriguez C, Health CW. Body mass index and mortality in a prospective cohort of U.S. adults. *New Eng J Med* 341:1097-1105; 1999.

CDC, *2005 Cancer incidence* – United States Cancer Statistics: 1999 - 2005 Incidence, WONDER On-line Database. United States Department of Health and Human Services, Centers for Disease Control and Prevention and National Cancer Institute; August 2008. Accessed at <http://wonder.cdc.gov/cancer-v2005.html> on Apr 23, 2010. *CDC, 2005 Cancer mortality* – United States Cancer Statistics: 1999 - 2005 Mortality, WONDER On-line Database. United States Department of Health and Human Services, Centers for Disease Control and Prevention; August 2008. Accessed at <http://wonder.cdc.gov/CancerMort-v2005.html> on Apr 23, 2010.

CDC-MMWR, Morbidity Weekly Report. Center of Disease Control 57:1226-1228; 2008. CDC, United States Department of Health and Human Services, How Tobacco Smoke Causes Disease: the Biology and Behavioral Basis for Smoking-Attributable Disease: A Report of the Surgeon General. Center for Disease Control, Atlanta GA, 2010.

Cucinotta, F.A.: Once we know all of the radiobiology we need to know how can we use it to predict risk and achieve fame and fortune. *Physica Medica XVII*: 5-12; 2001.

Cucinotta FA, Schimmerling W, Wilson JW, Peterson LE, Saganti P, Badhwar GD, Dicello JF. Space radiation cancer risks and uncertainties for Mars missions. *Radiat Res* 156:682–688; 2001.

Cucinotta FA, Kim MY, and Ren L. Evaluating shielding effectiveness for reducing space radiation cancer risks. *Radiat Meas* 41:1173-1185; 2006.

Cucinotta FA, Durante M. Cancer risk from exposure to galactic cosmic rays: implications for space exploration by human beings. *The Lancet Onc* 7: 431-435; 2006.

Cucinotta FA, Kim MY, Schneider SI, Hassler DM. Description of light ion production cross sections and fluxes on the Mars surface using the QMSFRG model. *Radiat Environ Biophys* 46: 101-106; 2007.

Cucinotta FA, Kim MH, Willingham V, George KA. Physical and biological organ dosimetry analysis for International Space Station Astronauts. *Radiat Res* 170:127–138; 2008.

Cucinotta FA, Chappell L. Updates to astronaut radiation limits: radiation risks for never-smokers. *Radiat Res* 176:102-114; 2011.

Cucinotta FA, Kim MY Chappell L. Space radiation cancer risk projections and uncertainties-2010. NASA TP 2011-216155; 2011.

Cucinotta FA, Chappell LJ, Kim MY, and Wang M. Radiation Carcinogenesis Risk Assessments for Never-Smokers. Submitted for publication, 2012.

DHHS (2002). U.S. Department of Health and Human Services. "42 CFR Part 81: 7868 Guidelines for determining the probability of causation under the Energy Employees Occupational Illness Compensation Program Act of 2000, Final Rule," 67 FR 22296–22314 (U.S. Government Printing Office, Washington).

Detours V, Wattel S, Venet D, Hutsebaut N, Bogdanova T, Tronko MD, Dumont JE, Franc B, Thomas G, and Maenhaut C. Absence of a specific radiation signature in post-Chernobyl thyroid cancers. *Br J Cancer* 92: 1545-1552; 2005.

Doll R, Peto R, Boreham J, and Sutherland I. Mortality in relation to smoking: 50 years' observations on male British doctors. *British Medical J* doi: 10.1136/bmj.38142.554479.AE; 2004.

Durante M, Cucinotta FA. Heavy ion carcinogenesis and human space exploration. *Nat Rev Cancer* 8:465-472; 2008.

Furukawa K, Preston DL, Lonn S, Funamoto S, Yonehara S, Takeshi M, et al. Radiation and smoking effects on lung cancer incidence among atomic bomb survivors. *Radiat Res* 174:72-82; 2010.

Gilbert ES, Stovall M, Gospodarowicz FE, van Leeuwen MFE, Andersson B, Glimelius, et al. Lung cancer after treatment for Hodgkin's disease: focus on radiation effects. *Radiat Res* 159:161-173; 2003.

IARC, International Agency for Research on Cancer. Tobacco smoking. IARC Monographs on the Evaluation of Carcinogenic Risks to Humans. Vol. 38. Lyon (France): IARC; 1986.

ICRP, *1990 Recommendations of the International Commission on Radiological Protection. ICRP Publication 60, Pergamon Press, Oxford, 1990.*

ICRP, *Relative Biological Effectiveness (RBE), Quality Factor (Q), and Radiation Weighting Factor (w_R). ICRP Publication 103. International Commission on Radiation Protection, Pergamon, 2003.*

Kim MY, George KA, and Cucinotta FA. Evaluation of skin cancer risks from lunar and Mars missions. *Adv Space Res* 37:1798-1803; 2006.

Kim MY, Hayat ML, Feiveson AH, and Cucinotta FA. Using high-energy proton fluence to improve risk prediction for consequences of solar particle events. *Adv Space Res* 44: 1428-1432; 2009.

Leigh WJ, Wakeford R. Radiation litigation and the nuclear industry - the experience in the United Kingdom. *Health Phys* 81: 646-654; 2001.

Leuraud K, Schnelzer M, Tomasek L, et al. Radon, smoking and lung cancer risk: results of a joint analysis of three European case-control studies among uranium miners. *Radiat Res* 176: 375-387; 2011.

Liang PS, Chen, TY, Giovannucci, E. Cigarette smoking and colorectal cancer incidence and mortality: Systematic review and meta-analysis. *Int J Cancer* 124: 2406-2415; 2009.

LSAH, Longitudinal Study of Astronaut Health Newsletter. Volume 12, 2003.
(http://lsda.jsc.nasa.gov/refs/LSAH/Vol_12_Issue_1_Jul_03.pdf).

Malarcher AM, Schulman J, Epstein LA, Thun MJ, et al. Methodological issues in estimating smoking-attributable mortality in the United States. *Am J Epidemiol* 152: 573-584; 2000.

NASA, Astronaut Fact Book, NP-2005-01-001 JSC, Houston TX, 2005.

NCRP, *Uncertainties in Fatal Cancer Risk Estimates Used in Radiation Protection*, National Council on Radiation Protection and Measurements Report 126: Bethesda MD, 1997.

NCRP. *Recommendations of Dose Limits for Low Earth Orbit*. National Council on Radiation Protection and Measurements Report 132: Bethesda MD; 2000.

NCRP, *Information Needed to Make Radiation Protection Recommendations for Space Missions Beyond Low-Earth Orbit*. National Council on Radiation Protection and Measurements Report No. 153: Bethesda MD, 2006.

NCRP. *Potential Impact of Individual Genetic Susceptibility and Previous Radiation Exposure on Radiation Risks for Astronauts*. National Council on Radiation Protection and Measurements Report 167: Bethesda MD; 2011.

Nikiforova MN, Rowland JM, Bove K, MonforteMunoz H, Fagin JA. Distinct patterns of ret oncogene rearrangements in morphological variants of radiation-induced and sporadic thyroid papillary carcinomas in children. *Cancer Res* 57: 1690-1694; 1997.

NIH. *Report of the NCI-CDC Working Group to Revise the 1985 NIH Radioepidemiological Tables*. NIH Publication No. 03-5387; 2003.

Pawel D, Preston DL, Pierce D, Cologne J. Improved estimates of cancer site-specific risks for A-bomb survivors. *Radiat Res* 169: 87-98, 2008.

Port M, Boltze C, Wang Y, Roper B, Meineke V and Abend M. A radiation-induced gene signature distinguishes post-Chernobly from sporadic papillary thyroid cancers. *Radiat Res* 168: 639-649; 2007.

Preston DL, Mattsson A, Holmberg E, Shore R, Hildreth NG, Boice JD. Radiation effects on breast cancer risk: a pooled analysis of eight cohorts. *Radiat Res* 158:220-235; 2002.

Preston DL, Ron E, Tokuoka S, Funamota S, Nishi N, Soda M, Mabuchi K, et al. Solid cancer incidence in atomic bomb survivors: 1958-1998. *Radiat Res* 168:1-64; 2007.

Ron E, Lubin JH, Shore RE, Mabuchi K, Modan B, Pottern L, Schneider AB, Tucker MA, Boice JD. Thyroid cancer after exposure to external radiation: a pooled analysis of seven studies. *Radiat Res* 141:259-277; 1995.

Sandler DP, Shore DL, Anderson JR, et al. Cigarette smoking and risk of acute leukemia: associations with morphology and cytogenetic abnormalities in bone marrow. *JNCI* 85:1994-2003; 2003.

Schimmerling W, Wilson JW, Cucinotta FA, Kim MH. Requirements for simulating space radiations with particle accelerators. In: *Risk Evaluation of Cosmic-Ray Exposure in Long-Term Manned Space Mission* (K. Fujitaka, H. Majima, K. Ando, H. Yasuda, and M. Susuki, Eds., Kodansha Scientific Ltd., Tokyo) 1-16, 1999.

SEER, Surveillance, Epidemiology, and End Results: Cancer Statistics Review, 2005. Cancer Surveillance Research Program, National Cancer Institute: Bethesda MD; 2006.

Storer JB, Mitchell TJ, Fry RJ. Extrapolation of the relative risk of radiogenic neoplasms across mouse strains and to man. *Radiat Res* 113: 331-353; 1988.

Thun MJ, Day-Lally C, Calle E, Flanders W, Heath C. Excess mortality among cigarette smokers: changes in a 20-year interval. *Am J Public Health* 85:1223–1230; 1995.

Thun MJ, Hannan LM, Adams-Campbell LL, Boffetta P, Buring JE, Feskanich D, et al. Lung cancer occurrence in never-smokers: an analysis of 13 cohorts and 22 cancer registry studies. *PLoS Med* 5:1357-1371; 2008

Travis LB, Curtis RE, Bennett WP, Hankey BF, Travis WD, Boice Jr JD. Lung cancer after Hodgkin's disease. *JNCI* 87:1324-1327; 1995.

Ugolin N, Ory C, Lefevre E, Behhabiles N, Hofman P, Schlumberger M, and Chevillard S. Strategy to find molecular signatures in a small series of rare cancers: validation for radiation-induced breast and thyroid tumors. *PLoS One* 6:1-14; 2011.

UNSCEAR, United Nations Scientific Committee on the Effects of Atomic Radiation, Sources and Effects of Ionizing Radiation. *UNSCEAR 2006 Report to the General Assembly, with Scientific Annexes*. New York: United Nations; 2008.

Weil MM, Bedford JS, Bielefeldt-Ohmann H, Ray AF, Gernik PC, Ehrhart EJ, Falgren CM, Hailu F, Battaglia CLR, Charles C, Callan MA, Ullrich RL. Incidence of acute myeloid leukemia and hepatocellular carcinoma in mice irradiated with 1 GeV/nucleon ⁵⁶Fe ions. *Radiat Res* 172:213-219; 2009.

Wilson JW, Townsend LW, Shinn JL, Cucinotta FA, Costen RC, Badavi FF, Lamkin SL. Galactic cosmic ray transport methods, past, present, and future. *Adv Space Res* 10: 841-852; 1994.